Recombination and population inversion in plasmas generated by tunneling ionization

G. J. Pert

Physics Department, University of York, Heslington, York YO10 5DD, United Kingdom

Above-threshold ionization (ATI) ionization by linearly polarized light has been proposed by several authors as a means of driving recombination lasers in the soft x-ray spectral region. The pump radiation generates a cold electron plasma with ions in a single ionization stage, which is an ideal starting condition for strong recombination. Population inversions form during the recombination cascade to the ground state of the next ionization stage. In the absence of any relaxation the electron distribution is strongly peaked near zero energy. However, a number of different processes all heat the cold electrons towards Maxwellian, and may thereby reduce the recombination rate in the higher levels. Using numerical models we investigate these relaxation processes and their effect on recombination. We show that the recombination can be well described by the standard cascade model, provided an appropriate temperature is used. We examine two cases in detail, hydrogen-like lithium where the inversion is with respect to the ground state, and lithium-like nitrogen where it is with respect to the first excited state. The two cases differ markedly in the degree of relaxation achieved, and in the duration of the population inversion.

PACS number(s): 52.50.Jm, 42.55.Vc, 32.30.Rj, 42.60.By

I. INTRODUCTION

There has been considerable interest for some years in the possibilities of generating x-ray laser action in the recombination cascade following high field tunneling ionization. The potential for this mechanism has been investigated by a number of authors following the original proposal by Burnett and Corkum [1] in 1989. Workable schemes have been proposed based on transitions to the ground and to the higher states. All these concepts rely on the very cold electron distribution generated following tunneling ionization by plane polarized light. Early calculations of the gain which could be generated by such an approach used electron Maxwell-Boltzmann energy distributions based on the mean energy [2]. However, as pointed out by Ditmire [3] the actual energy distribution of the electrons released by ionization is in fact strongly non-Maxwellian with very large values at low electron energy. Such a distribution strongly favors recombination and should enhance the generation of population inversion. Ditmire [3] showed that marked increases of the three body recombination rate to lower states should occur. More recently Avitzour *et al.* [4] have performed simulations on the recombination of hydrogen-like lithium ions and obtained significant population inversion and gain on the L_α transition to the ground state. Two distinct methodologies have been explored to generate gain through recombination based on tunneling ionization.

(i) The direct analogy of the early expansion cooled recombination lasers [5,6] in which the lower laser state is the first excited state state or higher. Such schemes operate in a quasi-steady mode through cascade recombination.

(ii) Following the approach of Peyraud and Peyraud [7], a direct transition to the ground state is used. Such an arrangement is obviously self-terminating and places stringent demands on the relative population rates of the states within the recombination process. It also requires that the ionization process itself leads to a very low population in the ground state at the end of the pump phase—a situation practically unachievable with thermal ionization, but realistic with photoionization.

Both these approaches rely on the characteristics of the recombination cascade through the excited states. Key to this behavior is the fact that collisional processes are strongest for small energy gaps, whereas radiative ones are favored by large jumps. Within the upper states transitions are, therefore, dominated by collisions between the bound and free electrons, in which the ion may be either excited or de-excited, the prevailing trend being downward. When the electron distribution is Maxwellian this rapidly leads to a Boltzmann distribution among the upper states in equilibrium with the free electrons. However, this thermal state can only be maintained down to a certain level, known as the "bottleneck" or "collision limit" depending on the nature of the transition across it. Below this level, the electrons de-excite freely by either collisions or radiation. This level being determined by the electron temperature. The rate of population to the lower states is determined by a random walk (diffusion) through the upper states [8–10] and by the nature of the subsequent decay. These processes were unified and cast into the framework of the collisional-radiative model by the author [11]. We shall need to return to this topic later.

Although the distribution generated following ionization by the laser is strongly non-Maxwellian there are important processes which drive the system towards equilibrium. These are all collisional and, therefore, operate most strongly on the slow electrons.

(i) Electron-electron collisions. This is the standard relaxation process tending to drive the electrons to a Maxwellian at the Spitzer equilibration rate. In our particular context where the distribution takes a particularly extreme form, the electron distribution tends to equilibrate most rapidly among the slower moving electrons, passing through a series of slowly heating quasi-Maxwellian distributions as the high energy tail is slowly drawn in.

(ii) Electron-ion collisions. During the laser pulse inverse bremsstrahlung absorption results from these collisions.

Again the interactions are dominantly with the slow electrons heating those in the low energy singularity to form a quasi-Maxwellian [12]. Once the laser pulse is switched off, this mechanism terminates.

(iii) Recombination of the slow moving electrons into upper-lying states, which will form the reservoir for the cascade, is accompanied by heating of the secondary electrons. The dominant electrons are slow and these are heated by energies corresponding to the upper states.

(iv) During the ionization process half the electrons will return to the neighborhood of the ion, where they will be scattered and gain further energy—in direct analogy with harmonic generation [13]. This process is not amenable to simple analysis. A number of electrons will be backscattered and may be released with high energy. However, if the density is high the quiver motion amplitude may be comparable with the ion separation, and an inverse bremsstrahlung collision will occur before the return. This process would then be included within the normal inverse bremsstrahlung description.

In this paper we will examine the recombination of plasma generated by tunneling ionization. The principal aim of this work is to investigate the nature of the relaxation and recombination in the cascade following tunneling ionization. To that end we have considered a short wavelength pump laser (0.25 μm) and hydrogen gas seeding to the primary gas, in order to obtain as cold an electron distribution as possible. Since hydrogen has only a single electron and a relatively low ionization potential, its energy at release is small. Hence adding a large fraction of hydrogen can substantially reduce the final electron temperature [2]. The results, although accurate, are intended to be explanatory, rather than predictive for any particular x-ray laser designs. We note that Avitzour and Suckewer in a recent paper [14] have also considered the pumping of hydrogenic lithium in the presence of a background of hydrogen, and shown significant gain may be generated.

Our principal tool will be the Fokker-Planck model developed earlier by the author [15] in which ionization, ion-electron, and electron-electron collisions are all modeled within a zero dimensional time dependent system. In particular we will examine the relaxation of the electron distribution towards Maxwellian and the simultaneous development of the population within the various excited states. In order to carry this out we will need to be able to accurately describe not only the free electron collisional processes, but also their interaction with those in the bound states. This will require that all transitions are carefully balanced by their reciprocal rate, through detailed balance relations. We, therefore, consider the development of these relations in some detail.

II. THE FOKKER-PLANCK APPROACH

Since this numerical technique will form the basis of our study, it is necessary to give a brief introduction to its application in this context.

We consider the electron distribution function, $f(v)$, in a one dimensional spherically symmetric velocity (or equivalently energy) space. In this case the time dependency due to

electron-electron collisions is described by the equation

$$\frac{\partial f}{\partial t} = \frac{1}{v^2} \frac{\partial}{\partial v} \left[\alpha f + \beta \frac{\partial f}{\partial v} \right] \quad (1)$$

where α and β are terms involving integrals of $f(v)$, whose forms are given in standard texts [16–18]. This equation is, therefore, nonlinear. It is assumed that the electron gas is dilute so that individual electron collisions are weak. This involves some implicit averaging over collision partners, in order to take into account the Coulomb logarithm. This approximation is satisfactory when the distribution is nearly Maxwellian. However, it may lead to error in more general cases [19] when this average may lead to an increase in the relaxation rate. However, the level of error can be checked either by Monte Carlo calculation [20] or by molecular dynamic simulation [19], when each collision partner is treated individually without averaging.

If the ions are assumed heavy and stationary, electron-ion collisions only give rise to collisional absorption and, therefore, heating of the electrons during the laser pulse. Assuming the individual energy impulses given to an electron are small, this process can also be described by a Fokker-Planck expression.

$$\frac{\partial f}{\partial t} = \frac{1}{v^2} \frac{\partial}{\partial v} \left\{ \frac{u_0^2}{v^2} \frac{\partial}{\partial v} [\ln[\Lambda(v)]R(v)f(v)] + \frac{v^2}{u_0} \frac{\partial}{\partial v} [S(\Delta,v)f(v)] \right\}. \quad (2)$$

The functions $R(v)$, $S(\Delta,v)$, the appropriate Coulomb logarithm for absorption $\ln(\Lambda(v))$ and its multiplying factor Δ are given in an earlier work [15].

The development of the electron distribution proceeds as an initial value problem, in which the velocity distribution is defined on a finite difference mesh. The initial ionization is carried out by assigning an appropriate probability to each cell in accordance with the ionization rate at that time. The calculations are reasonably straightforward involving nonlinear diffusion in velocity space. As the system of finite difference equations are not fully conservative, there is a slow total energy change [15]. Since this error is second order it can be reduced by using a sufficiently large number of cells, and is not a problem in the cases considered here, where we have used 400 cells on a nonuniform velocity mesh.

III. INELASTIC COLLISIONS

We now turn to the problem of treating inelastic collisions. In this case the energy exchange is no longer small and we cannot continue to use a Fokker-Planck formalism, but must treat the problem within a Boltzmann collision framework. Numerically this entails exchanging electrons between the various velocity (or energy) cells according to the respective energy overlaps and probability. This is not a trivial problem, particularly for ionization and three-body recombination, if it is required that both energy conservation and detailed balance be maintained, as is essential if equilibrium is to be attained. We consider first the simpler case of excitation/de-excitation. We assume that the electron cross section for excitation is known as a function of the colliding
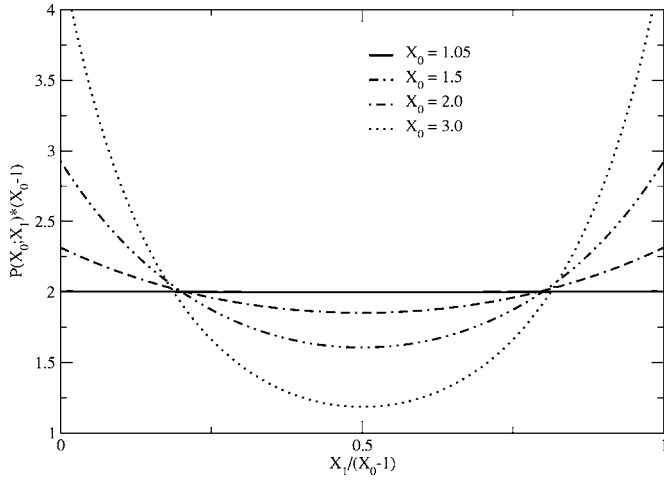
FIG. 1. Plots of the normalized form of the differential ionization probability function $P(X_0;X_1)(X_0-1)$ for the classical model as function of the normalized incoming electron energy, X_0 and the energy of one of the outgoing electrons as a fraction of the energy, excess $X_1/(X_0-1)$.

electron energy. Hence we may calculate the upward rate per unit volume for the transition from the state 1 of energy E_1 to the state 2 of energy E_2 by electrons of energy ϵ_1 as $R_{12}(E_1,\epsilon_1)n_1n_e(\epsilon_1)d\epsilon_1$, where n_1 is the density of ions in the state 1 and $n_e(\epsilon_1)d\epsilon_1=n_ef(v_1)4\pi v_1^2 dv_1$ is the density of free electrons in the energy range $(\epsilon_1,d\epsilon_1)$. The reciprocal rate for de-excitation is given by an identical term $R_{21}(E_2,\epsilon_2)n_2n_e(\epsilon_2)d\epsilon_2$. When the energies are related by the conservation of energy, the processes are reciprocal and the principle of detailed balance [21] requires the relation:

$$R_{12}(E_1,\epsilon_1)g_1[\rho(\epsilon_1)d\epsilon_1]=R_{21}(E_2,\epsilon_2)g_2[\rho(\epsilon_2)d\epsilon_2] \quad (3)$$

where g_1 and g_2 are the statistical weights of states 1 and 2, respectively, and $\rho(\epsilon)$ is the density of free electron states per unit volume:

$$\rho(\epsilon) = \frac{4\pi(2m_e)^{3/2}}{h^3}\epsilon^{1/2}. \quad (4)$$

The conservation of energy requires that $E_1+\epsilon_1=E_2+\epsilon_2$ and that $d\epsilon_1=d\epsilon_2$. The symmetric nature of the process is clearly demonstrated by writing Eq. (3) in the form:

$$R_{12}(E_1,\epsilon_1)g_1\rho(\epsilon_1)\delta(E_1+\epsilon_1-E_2-\epsilon_2)d\epsilon_1d\epsilon_2$$
$$= R_{21}(E_2,\epsilon_2)g_2\rho(\epsilon_2)\delta(E_2+\epsilon_2-E_1-\epsilon_1)d\epsilon_2d\epsilon_1. \quad (5)$$

Ionization and its inverse process—direct three body recombination—are more difficult. We must assume that the detailed ionization cross section giving the probability of the individual electron speeds on release is known. In fact in most cases this is not available but the total cross section is known and some approximation as to the relative distribution between the two electrons must be made, for example, based on the classical model. To develop the reciprocal rates consider ionization by an electron of energy $(\epsilon_0,d\epsilon_0)$ yielding electrons of energy $(\epsilon_1,d\epsilon_1)$ and $(\epsilon_2,d\epsilon_2)$. We may write the

ionization rate from a state of energy E_0 to one of energy E_1 in the form:

$$R_+(E_0,\epsilon_0;E_1,\epsilon_1,\epsilon_2)n_0n_e(\epsilon_0)\delta(E_1+\epsilon_1+\epsilon_2-E_0-\epsilon_0)d\epsilon_0d\epsilon_1d\epsilon_2$$
$$(6)$$

and the recombination rate is

$$\tfrac{1}{2}R_-(E_1,\epsilon_1,\epsilon_2;E_0,\epsilon_0)n_1n_e(\epsilon_1)n_e(\epsilon_2)$$
$$\delta(E_1+\epsilon_1+\epsilon_2-E_0-\epsilon_0)d\epsilon_0d\epsilon_1d\epsilon_2. \quad (7)$$

The factor $\tfrac{1}{2}$ takes into account the double counting associated with the indistinguishability of the electrons, ϵ_1 and ϵ_2, implied within the integration over the $\delta(\ )$ function. The equation of balance applied to these rates yields the following reciprocal relationship:

$$g_0[\rho(\epsilon_0)d\epsilon_0]R_+(E_0,\epsilon_0;E_1,\epsilon_1,\epsilon_2)d\epsilon_1d\epsilon_2$$
$$= g_1[\rho(\epsilon_1)d\epsilon_1][\rho(\epsilon_2)d\epsilon_2]R_-(E_1,\epsilon_1,\epsilon_2;E_0,\epsilon_0)d\epsilon_0. \quad (8)$$

Introducing the ionization potential $I=E_1-E_0$ and integrating over ϵ_2, the number of three body recombinations per unit volume per unit time can therefore be written as

$$\frac{h^3}{4\pi(2m_e)^{3/2}}\frac{g_0}{g_1}n_1n_e^2\int_I^\infty d\epsilon_0\int_0^{(\epsilon_0-I)/2}d\epsilon_1$$
$$\times\frac{\epsilon_0^{1/2}}{\epsilon_1^{1/2}(\epsilon_0-I-\epsilon_1)^{1/2}}f(\epsilon_1)f(\epsilon_0-I-\epsilon_1)$$
$$\times R_+(E_0,\epsilon_0;E_1,\epsilon_1,(\epsilon_0-I-\epsilon_1)) \quad (9)$$

where $f(\epsilon)$ is the energy probability distribution function and n_e the total electron density.

In thermal equilibrium, when the electron distribution is Maxwellian,

$$f(\epsilon) = \frac{4\sqrt{2}\pi}{(2\pi kT_e)^{3/2}}\epsilon^{1/2}\exp\left(-\frac{\epsilon}{kT_e}\right) \quad (10)$$

and the ion distribution is given by Saha's equation:

$$\frac{n_1n_e}{n_0} = 2\frac{(2\pi m_e kT_e)^{3/2}}{h^3}\frac{g_1}{g_0}\exp\left(-\frac{I}{kT_e}\right) \quad (11)$$

Eq. (9) reduces to the total ionization rate per unit volume per unit time, in accordance with the familiar detailed balance relation, i.e.

$$n_0\int_I^\infty d\epsilon_0\int_0^{(\epsilon_0-I)/2}d\epsilon_1 f(\epsilon_0)R_+(E_0,\epsilon_0;E_1,\epsilon_1,(\epsilon_0-I-\epsilon_1)).$$
$$(12)$$

If the released electrons are distributed uniformly in energy with one electron in the range $0<\epsilon_1<(\epsilon_0-I)/2$, the ionization rate may be written in the simpler form

$$R_+(E_0,\epsilon_0;E_1,\epsilon_1,\epsilon_2) = \frac{2}{(\epsilon_0-I)}\bar{R}_+(E_0,\epsilon_0;E_1). \quad (13)$$

This condition is implicit in the expression given by Lee [3], where $\bar{R}_+(E_0,\epsilon_0;E_1)$ is the net ionization rate for electrons of

energy ϵ_0 between the levels E_0 and E_1, for example, given by the Lotz approximation [22].

Unlike the situation with excitation between two bound levels where the energy of the electron after collision is uniquely determined, ionization has a continuum final state where the energy is divided in some ratio between two electrons. If we can identify the probability that the electron energies are divided in some ratio, we may use well-known results for the total ionization rate by electrons of energy ϵ_0 to obtain the required value. We define the probability that the energy of electron 1 is in the range $(\epsilon_1, d\epsilon_1)$ by $P(X_0; X_1)dX_1$ where $X_i = \epsilon_i/(E_1 - E_0)$ are the electron energies normalized to the ionization energy. Clearly this function must be symmetric with respect to the interchange of electrons 1 and 2, and $X_0 = 1 + X_1 + X_2$. Unfortunately this probability is not generally expressible by a simple algebraic relationship. Very close to threshold we may argue that since the bound and continuum states form a continuous sequence, the probability of the electron ϵ_0 exciting the atom to a particular state is given by a continuous function of the overall energy. Thus if the initial electron energy is near the ioniza-

tion threshold, $\epsilon_0 \sim I = E_1 - E_0$ this probability may be expressed by a Taylor's series:

$$R_+(E_0, \epsilon_0; E_1, \epsilon_1, \epsilon_2) = R_+(E_0, \epsilon_0; E_1, 0, (E_0 + \epsilon_0 - \epsilon_1))$$
$$+ \epsilon_1 \left. \frac{dR_+(E_0, \epsilon_0; E_1, \epsilon_1, \epsilon_2)}{d\epsilon_1} \right|_{\epsilon_0 = 0}.$$
$$(14)$$

For sufficiently small variations in $\epsilon_1 \ll \epsilon_0 \sim I$, the ionization rate is nearly constant, and independent of the value of the energies of the scattered or released electrons. Hence since one electron must be found in the energy range $0 < \epsilon_1 < \frac{1}{2}(\epsilon_0 - I)$ near threshold the probability of a release energy $(\epsilon_1, d\epsilon_1)$ is simply $2d\epsilon_1/(\epsilon_0 - I)$; or $P(X_0; X_1)dX_1 \approx 2dX_1/(X_0 - 1)$. This is a useful result for consideration of OFI pumped recombination lasers, where the electrons are necessarily cold.

Extending to higher energies in the neighborhood of the threshold, we may use the classical impulse model [23] and obtain the result:

$$P(X_0; X_1)dX_1 = 2 \frac{\left\{ \frac{1}{(1 + X_1)^2} \left[1 + \frac{4}{3(1 + X_1)} \right] + \frac{1}{(1 + X_2)^2} \left[1 + \frac{4}{3(1 + X_2)} \right] - \frac{1}{(1 + X_1)(1 + X_2)} \right\}}{\left\{ \left(1 - \frac{1}{X_0} \right) + \frac{2}{3} \left(1 - \frac{1}{X_0^2} \right) - \frac{1}{1 + X_0} \ln X_0 \right\}} dX_1. \quad (15)$$

The essential symmetry between the two outgoing electrons is clearly seen. Figure 1 shows plots of this function for various values of X_0 and the outgoing electron energy as a fraction of the energy excess $X_1/(X_0 - 1)$. It is clearly seen that for $X_0 \lesssim 2$ the probability is nearly constant. Far from threshold $(X_0 \gg 1)$ the Born approximation is valid and $P(X_0; X_1) \sim X_1^3 dX_1/(1 + X_1)^4$. If the total ionization rate, $\bar{R}_+(E_0, \epsilon_0; E_1)$ is given by some appropriate source [22,24] then the required rate can be written as

$$R_+(E_0, \epsilon_0; E_1, \epsilon_1, \epsilon_2) = I \bar{R}_+(E_0, \epsilon_0; E_1) P(X_0; X_1). \quad (16)$$

A. Ionization rate

The nature of the ionization process differs somewhat from one application to another. For collisional systems the electrons are hot, and empirical models based on the Bethe approximation [22] or the Born approximation [24] can be used. On the other hand the electrons are necessarily cold for recombination lasers, and the ionization is near threshold. Unfortunately the behavior near threshold still remains poorly understood in that few general results are available. Wannier's [25] analysis showed that the energy scaling was slightly stronger than linear, i.e., the rate scaled as $(\epsilon_0 - I)^{1.1}$.

However, although the result gave the scaling, the actual value remained undefined. At these low energies it can be argued that the classical impact model should give reasonable accuracy when correctly symmetrized and with exchange included [23]. The model can be further extended to include higher energy collisions through the introduction of the impact parameter formulation (ECIP) [26] to be consistent in all regimes. In this work for studying recombination in cold plasma we shall use the classical impact model alone.

B. Numerical integration

The treatment of excitation and ionization is relatively straightforward within the finite difference scheme. The Fokker-Planck algorithm [15] considers energy space divided into a series of cells of width $\Delta\epsilon$, which define the mesh. The energy of the upper boundary of the cell i is given by the recursion $\epsilon'_{i+1/2} = \epsilon'_{i-1/2} + \Delta\epsilon_i$ subject to $\epsilon'_{-1/2} = 0$. The energy of the cell is taken as the mean value of the boundary values, namely $\epsilon_i = \frac{1}{2}(\epsilon'_{i-1} + \epsilon'_i)$. We assume the electrons are distributed uniformly within the cell. Following excitation or ionization we need to re-assign the electrons to cells overlapping in energy taking into account the energy change in the atomic system, i.e., the bound electrons, in such a way that the total energy is conserved.

Thus if we consider the excitation of electrons from the energy group ϵ_1 of width $\Delta\epsilon_1$, the resulting electron may fall in one of a number of energy groups, $\epsilon_2 = E_1 + \epsilon_1 - E_2$ of width $\Delta\epsilon_2$, within the energy range $\Delta\epsilon_1$. The fraction of the resultant rate, which is assigned to a particular final energy group $(\epsilon_j, \Delta\epsilon_j)$, may be defined by a transfer weight assuming a uniform distribution over the interval. In order to satisfy the condition of detailed balance the weight $w_{i,j}$ assigned to a transition from a cell $(\epsilon_i, \Delta\epsilon_i)$ to $(\epsilon_j, \Delta\epsilon_j)$ must match the reverse $w_{j,i}$ from $(\epsilon_j, \Delta\epsilon_j)$ to $(\epsilon_i, \Delta\epsilon_i)$. The easiest way to set up this reciprocal relation is to re-write the rates in the symmetric form: $\int R_{12}(E_1, \epsilon_1) n_1 n_e(\epsilon_1) \delta(E_1 + \epsilon_1 - E_2 - \epsilon_2) d\epsilon_1 d\epsilon_2$. The symmetric weight is then obtained by integrating this equation over the mesh intervals $(\epsilon_i, \Delta\epsilon_i)$ and $(\epsilon_j, \Delta\epsilon_j)$, i.e.,

$$w_{i,j} \Delta\epsilon_i \Delta\epsilon_j = \int_{\epsilon_i - \Delta\epsilon_i/2}^{\epsilon_i + \Delta\epsilon_i/2} d\epsilon_1 \int_{\epsilon_j - \Delta\epsilon_j/2}^{\epsilon_j + \Delta\epsilon_j/2} d\epsilon_2 \, \delta(E_1 + \epsilon_1 - E_2 - \epsilon_2).$$

$$(17)$$

Since $w_{i,j}$ is symmetric suppose $\Delta\epsilon_j > \Delta\epsilon_i$ and let ϵ be the energy mismatch $\epsilon = |E_1 + \epsilon_i - E_2 - \epsilon_j|$, then

$$w_{i,j} = \begin{cases} 1/\Delta\epsilon_i & \text{when } \epsilon < \tfrac{1}{2}(\Delta\epsilon_j - \Delta\epsilon_i) \\ \left(\tfrac{1}{2}[\Delta\epsilon_j + \Delta\epsilon_i] - \epsilon\right)/(\Delta\epsilon_j \Delta\epsilon_i) & \text{when } \tfrac{1}{2}(\Delta\epsilon_j - \Delta\epsilon_i) < \epsilon < \tfrac{1}{2}(\Delta\epsilon_j + \Delta\epsilon_i) \\ 0 & \text{when } \tfrac{1}{2}(\Delta\epsilon_j + \Delta\epsilon_i) < \epsilon \end{cases}$$

$$(18)$$

It is easy to see that this function $w_{i,j}$ is just the overlap of cell i with j taking into account the mismatch.

The calculation of the rates for ionization/recombination is carried out in a similar fashion, but with the rates integrated over the three cells of width $\Delta\epsilon_i$, $\Delta\epsilon_j$, and $\Delta\epsilon_k$ to yield a reciprocal weight function $w_{i,j,k}$ to be used to assign the contributions following collision. Thus given three cells centered at ϵ_i, ϵ_j, and ϵ_k, respectively, such that $\Delta\epsilon_k > \Delta\epsilon_j > \Delta\epsilon_i$ and integrating over the appropriate intervals in Eqs. (6) and (7), we may write the probability of a transition per ion per electron per unit time between the three cells in the form $R(E_0, E_1, \epsilon_i, \epsilon_j, \epsilon_k) w_{i,j,k} \Delta\epsilon_i \Delta\epsilon_j \Delta\epsilon_k$. The value of weight function $w_{i,j,k}$ is given by

$$w_{i,j,k} = \begin{cases} \left\{1/\Delta\epsilon_k - \left\{\epsilon^2 + \tfrac{1}{2}(\Delta\epsilon_k - \Delta\epsilon_j - \Delta\epsilon_i)^2\right\}/(\Delta\epsilon_i \Delta\epsilon_j \Delta\epsilon_k)\right\} \text{ if } (\Delta\epsilon_k - \Delta\epsilon_j - \Delta\epsilon_i < 0) \\ \qquad \text{when } 0 < \epsilon < \tfrac{1}{2}|\Delta\epsilon_k - \Delta\epsilon_j - \Delta\epsilon_i| \\ 1/\Delta\epsilon_k - \tfrac{1}{2}\left(\tfrac{1}{2}(\Delta\epsilon_k - \Delta\epsilon_j - \Delta\epsilon_i) - \epsilon\right)^2/(\Delta\epsilon_i \Delta\epsilon_j \Delta\epsilon_k) \\ \qquad \text{when } \tfrac{1}{2}|\Delta\epsilon_k - \Delta\epsilon_j - \Delta\epsilon_i| < \epsilon < \tfrac{1}{2}(\Delta\epsilon_k - \Delta\epsilon_j + \Delta\epsilon_i) \\ \left\{\tfrac{1}{2}(\Delta\epsilon_j + \Delta\epsilon_k) - \epsilon\right\}/(\Delta\epsilon_j \Delta\epsilon_k) \\ \qquad \text{when } \tfrac{1}{2}|\Delta\epsilon_k - \Delta\epsilon_j + \Delta\epsilon_i| < \epsilon < \tfrac{1}{2}(\Delta\epsilon_k + \Delta\epsilon_j - \Delta\epsilon_i) \\ \tfrac{1}{2}\left\{\tfrac{1}{2}(\Delta\epsilon_k + \Delta\epsilon_j + \Delta\epsilon_i) - \epsilon\right\}^2/(\Delta\epsilon_i \Delta\epsilon_j \Delta\epsilon_k) \\ \qquad \text{when } \tfrac{1}{2}(\Delta\epsilon_k + \Delta\epsilon_j - \Delta\epsilon_i) < \epsilon < \tfrac{1}{2}(\Delta\epsilon_k + \Delta\epsilon_j + \Delta\epsilon_i) \\ 0 \qquad \text{when } \tfrac{1}{2}|\Delta\epsilon_k + \Delta\epsilon_j + \Delta\epsilon_i| < \epsilon \end{cases}$$

$$(19)$$

where $\epsilon = |E_0 + \epsilon_i - E_1 - \epsilon_j - \epsilon_k|$ is the energy mismatch.

Radiative recombination is easily included within this framework.

IV. ELECTRON TUNNELING IONIZATION

In the absence of re-scattering, immediately following ionization in an oscillating electric field at phase angle ϕ, $E = E_0 \sqrt{\tfrac{1}{2} + (\chi + \tfrac{1}{2}\cos(2\phi)}$, the probability per unit time of an electron being released with energy $(\epsilon, d\epsilon)$ can be written approximately as

$$p(\epsilon) d\epsilon = \frac{P_0(\epsilon_q/(\epsilon_q - \epsilon))^{(n^* - 1/2|m| - 1/2)}}{\pi\sqrt{\left[\left(\chi - \tfrac{1}{2}\right)^2 - \left(\tfrac{1}{2} - \epsilon/\epsilon_q\right)^2\right]}}$$

$$\times \exp\left[\alpha\left(1 - \sqrt{\epsilon_q/(\epsilon_q - \epsilon)}\right)\right] \frac{d\epsilon}{\epsilon_q} \qquad (20)$$

where χ is the polarization parameter ($\chi = 0$ or 1 linear and $\chi = \tfrac{1}{2}$ circular), $\epsilon_q = eE_0/(2m_e\omega^2)$ the peak quiver energy, $E_0 = (8\pi I/c)^{1/2}$ is the peak electric field, I and ω being the intensity and angular frequency of the field. The probability constant for a state (n^*, l, m) is given by Perelomov et al. [27].

$$P_0 = \frac{\omega_{at}}{2} C_{n^*}^2 \frac{I}{I_h} \frac{(2l+1)(l+|m|)!}{2^{|m|}(|m|)!(l-|m|)!}$$

$$\times \left[2\left(\frac{I}{I_h}\right)^{3/2} \frac{E_{at}}{E_0} \right]^{(2n^*-|m|-1)}$$

$$\times \exp\left\{ -\frac{2}{3}\left[\frac{E_{at}}{E_0}\right]^{(2n^*-|m|-1)} \right\} \qquad (21)$$

where the atomic units of frequency and electric field are, respectively, ω_{at} and E_{at}, the effective quantum number $n^* = Z(I_h/I)^{1/2}$ for an ion of charge $(Z-1)$ and the constant $C_{n^*} \approx (2e/n^*)^{n^*}(2\pi n^*)^{-1/2}$ is given by Ammosov *et al.* [28]. The constant α in Eq. (20) is determined by the argument of the exponential in Eq. (21) namely

$$\alpha = \frac{2}{3}\left(\frac{I}{I_h}\right)^{3/2} \frac{E_{at}}{E_0}. \qquad (22)$$

A. Circular polarization

For circular polarization $\chi = \frac{1}{2}$ this reduces Eq. (20) to the simple form

$$p(\epsilon)d\epsilon = P_0 2^{(n^*-1/2|m|-1/2)} \exp[\sqrt{2}-1]\alpha]\delta(\epsilon - \epsilon_q/2)d\epsilon \qquad (23)$$

since all electrons are released with energy $\frac{1}{2}\epsilon_q$.

B. Linear polarization

For linear polarization we obtain

$$p(\epsilon)d\epsilon = \frac{P_0[\epsilon_q/(\epsilon_q-\epsilon)]^{(n^*-1/2|m|-1/2)}}{\pi\sqrt{[(\epsilon/\epsilon_q)(1-\epsilon/\epsilon_q)]}}$$

$$\times \exp[\alpha(1-\sqrt{\epsilon_q/(\epsilon_q-\epsilon)})]\frac{d\epsilon}{\epsilon_q} \qquad (24)$$

which, as noted elsewhere [3,4], diverges as $\epsilon \to 0$.

For $n^* = 1$ the probability of an electron being released with phase $(\phi, d\phi)$ is

$$p(\phi)d\phi = P_0 \exp(\alpha)\sec\phi \exp[-\alpha\sec\phi]d\phi \qquad (25)$$

and hence the probability per unit time averaged over the full cycle can be evaluated in terms of standard functions

$$\bar{p} = \frac{2}{\pi}P_0 \exp(\alpha)K_0(\alpha) \qquad (26)$$

and the average electron energy

$$\bar{\epsilon} = \frac{2}{\pi}\frac{P_0}{\bar{p}} \exp(\alpha)\{K_0(\alpha) + \alpha[Ki_1(\alpha) - K_1(\alpha)]\}\epsilon_q$$

$$= \left\{ 1.0 + \frac{\alpha[Ki_1(\alpha) - K_1(\alpha)]}{K_0(\alpha)} \right\}\epsilon_q \qquad (27)$$

where $K_0(z)$ and $K_1(z)$ are modified Bessel functions of the zero and first order and $Ki_1(z)$ is the integral of $K_0(z)$. For

large α, i.e., near threshold, these expressions take a simple form:

$$\bar{p} \approx \sqrt{\frac{2}{\pi\alpha}}P_0 \quad \text{and} \quad \bar{\epsilon} \approx \frac{1}{\alpha}\epsilon_q. \qquad (28)$$

Since the emission is dominantly at the field maximum, $E \approx E_0(1-\phi^2/2)$, these asymptotic forms are valid to lowest order in $1/\alpha$ for arbitrary n^*.

1. Re-scattering

In a linearly polarized field, if the electron phase lies between 0 and $\pi/2$, or π and $3\pi/2$, the electron will return to the neighborhood of the ion on the next half-cycle, where it will be scattered resulting in a deflection and a further thermal energy gain; thereby removing the singularity in the distribution for half the electrons.

We may attempt to take rescattering into account by the following quasi-classical argument [29,30]. The electron escapes from the ion by tunneling at a phase angle ϕ. The returning electron has a classical motion, which interacts with the ion at phase angle ψ given by:

$$\cos\psi + (\psi - \phi)\sin\phi - \cos\phi = 0 \qquad (29)$$

when the velocity is

$$v = v_\psi - v_\phi = v_q[\sin\psi - \sin\phi] \qquad (30)$$

where $v_q = eE_0/(m\omega)$ is the maximum quiver speed. Note the similarity of this process with that invoked to explain the plateau region of high harmonic generation [13], whose limit corresponds to release at phase angle $\phi = 0.313$ and return at $\psi = 4.399$: The corresponding energy change being $1.587\epsilon_q$. The harmonic process is completed by recombination. In contrast in our case it is followed by elastic scattering.

Within an impact approximation, we may imagine that the electron at this point is scattered by the ion through some angle θ. The new velocity has components $v_x = v\cos\theta$ and $v_y = v\sin\theta$. The "thermal" velocity is obtained by subtracting the quiver term v_ψ. The thermal energy is, therefore

$$\epsilon = \frac{1}{2}m_e[(v_x - v_\psi)^2 + v_y^2]$$

$$= m_e v_q^2 \left\{ \sin\psi(\sin\psi - \sin\phi)(1-\cos\theta) + \frac{1}{2}\sin^2\phi \right\}. \qquad (31)$$

To proceed further requires knowledge of the scattering angle θ. In principle we may consider that the electron at release has a wave-packet whose lateral spread is given by the distribution of transverse momentum. This was found by Delone and Krainov [31] to be Gaussian, which may be interpreted as a wave packet of spatial width $\left(\frac{I}{I_H}\right)^{1/4}\left(\frac{E_a}{E_0}\right)^{1/2}a_0$. Following Paulus *et al.* [29], this may be used to determine a scattering probability using the classical formula for Rutherford scattering. We may note that typically the scaling with ionic charge Z requires $I \sim Z^2$ and $E_0 \sim Z$ so that the wave packet width is typically $3a_0$, i.e., of the order of the atomic dimensions. However, the electron wavelength at the quiver
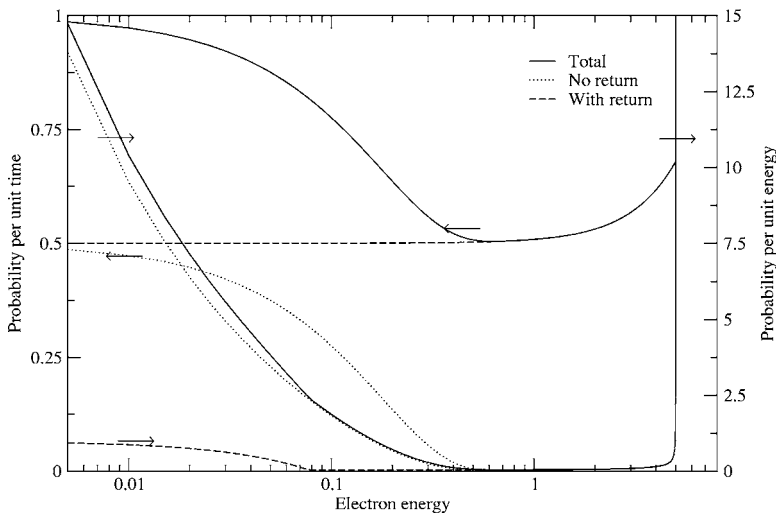
FIG. 2. Plot of the probability of emission in terms of P_0 as a function of the electron energy showing both the probability per unit time and the energy differential probability. The parameter $\alpha=12$.

speed $\lambda \approx \frac{\hbar\omega}{I_H}\frac{E_a}{E_0}a_0$ will also be of the order of Bohr radius a_0. As a result the collision is strong and it will be sufficient for our purposes to consider only the case of backscattering, where $\theta=\pi$. The probability distribution of the phase angle ϕ is given by Eq. (20), when ψ is obtained from Eq. (29) and hence the energy from Eq. (31). As has already been pointed out elsewhere [29,30] this leads to a substantial enhancement of the electron energy up to a maximum value of $5.036\epsilon_q$, which occurs at an initial phase angle $\phi=0.263$ and rescattering at angle $\psi=4.56$. Figure 2 shows both the probability of release per unit time and the energy differential probability both as fractions of P_0 as a function of the electron energy, when $n^*=1$ and $\alpha=12$. The plot is clearly divided into two distinct parts. At low electron energies direct release without scatter is dominant, whereas the high energy part is due to rescattering. The sharp cutoff and discontinuity at peak energy is a direct consequence of the zero gradient at the maximum, and is smoothed out in a more accurate calculation [30]. This graph, taken at a typical value of α, clearly illustrates the essential nature of the re-scattering process leading to much higher energies for 50% of the electrons.

However, when the ambient density is sufficiently high, the background fields deflect the electron before it returns to the ion sufficiently strongly to avoid strong coherent scattering. Since only a small angle of scatter is required (due to the small spatial size of the wave packet) to prevent the backscattering, re-scattering is much less effective at the densities appropriate to generating x-ray laser action. In this case the behavior is identical to the normal ion scattering which gives rise to inverse bremsstrahlung scattering, and is already treated within our modeling. We shall assume that this is the case here. It is interesting to reflect that our primary aim is to avoid generating too many "hot" electrons it may be advisable to maintain a sufficiently high background density to destroy the coherence of the motion of the returning electrons.

Alternatively since the hot electrons formed by rescattering have energies greatly in excess of those from primary emission, they will be seen to play no role in the recombination process, apart from possibly weakly ionizing the ground state. For the purpose of estimating recombination, we may discount this process (if it is important) but note that there may be an effective reduction of the electron density by nearly 50%.

V. HYDROGEN-LIKE LITHIUM (LI III)

As an example of a ground state recombination system we consider recombination to the hydrogen-like lithium ion. The laser pulse is taken to have a peak power of 10^{17} W cm^{-2} in a pulse of duration 100 fs at wavelength 0.254 μm. To improve the cooling of the gas we consider a mixture of 10% lithium with 90% hydrogen at a total atom density of 10^{19} cm^{-3} [2].

The hydrogen-like lithium ion is treated with a set of hydrogen levels with the principal quantum number n in the range of 1–10. At these fields both the hydrogen and lithium are fully stripped. The hydrogen ionization occurs early on the rising edge of the pulse, together with the early ionization stage of the lithium. The later stages of lithium ionization occur near the peak of the pulse. Thus we may conclude that the electrons produced by the ionization of hydrogen and the 2s state of Li I are relatively cold, whereas those from Li II and Li III are hot. Since the fraction of lithium is relatively small, the bulk of the electrons are cold. This behavior accounts for the structure seen in Fig. 3(a).

A. Electron distribution

The electron distribution function due solely to the ATI heating, shown in Fig. 3(a), confirms these expectations. Comparing the distribution with the Maxwellian based on the mean energy, we can see that the distribution is strongly nonequilibrium, with a discontinuity at zero energy and a substantial hot electron tail. However, the introduction of collisional effects rapidly makes a significant difference to the distribution [Fig. 3(b)] by the end of the pulse. The low energy discontinuity is removed and it can be seen that the distribution is nearly Maxwellian (except in the high energy tail), but defined by the mode energy, given by the maximum of the actual distribution rather than by the mean, which is strongly affected by the energy in the tail.
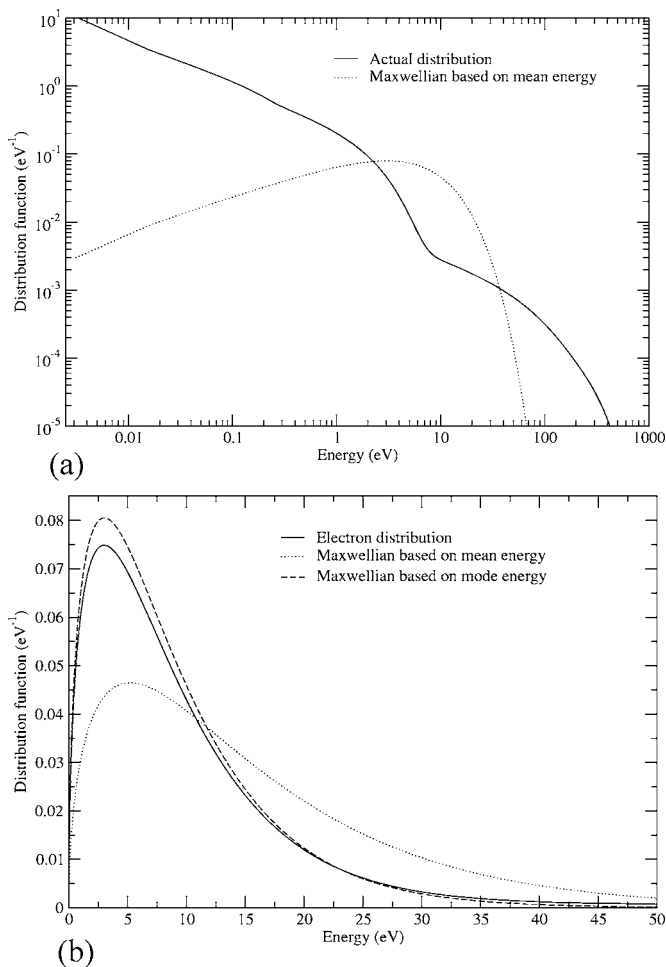
(a)

(b)

FIG. 3. Plots of the electron distribution function at the end of the pump pulse for (a) pure ATI heating only and (b) with electron collisions.

We now examine the development of the distribution with time in Fig. 4, observing the progressive development of a Maxwellian towards that defined by the mean electron energy.

We note that by 2.5 ps after the end of the pulse, relaxation to the mean energy is nearly complete. Since the energy of peak of the Maxwellian based on the mean energy is always larger than that of the actual distribution based on the same total electron energy, we note that the form of the distribution at high energies falls off more slowly than the Maxwellian, up the maximum value allowed by the quiver motion, as exemplified in Fig. 3(a). Although these electrons are small in number they possess a large proportion of the total energy as evidenced by the difference between the mode and mean energies. The hotter electrons will play no role in the recombination.

B. Electron relaxation

Relaxation is the result of three distinct effects, which we will now investigate individually, including each alone in the development of the plasma by switching off the relevant terms in the code:

(i) Electron-electron collisions. This is the dominant effect leading to a Maxwellian distribution and continues until relaxation is complete. It can be seen [Fig. 5(a)] that even during the pulse it is effective removing the singularity in the distribution at zero velocity. This is a consequence of the fact that the collision frequency of the slow electrons is much larger than that of the fast. This is further reflected in the slow thermalization of the hot tail still remaining at the later time [Fig. 5(b)].

(ii) Electron-ion collisions. These are the energy absorbing, inverse bremsstrahlung collisions, which are only effective during the laser pulse. They also heat the slow electrons preferentially, and hence again the zero energy singularity is eliminated (Fig. 6). The electron heating is shown by the increase in the value of the mean energy from 8.6 eV to 15.2 eV. Since the laser quiver energy is much larger than the mean, the distribution would achieve a (nonisotropic) Maxwellian [12]. In this simulation it is assumed that isotropization is rapid due to electron-ion and electron-electron collisions once the field is switched off, and the distribution may, therefore, be treated as isotropic. The clear Maxwellian form of the distribution about the mode is readily seen, with the high energy tail relatively unchanged.

(iii) Electron recombination re-heat. As three-body recombination proceeds the spectator electron gains energy from the recombination. Since three body recombination is strongest for the low energy electrons, the electron distribution exhibits a series of peaks corresponding to the individual energy levels in the ion immediately following the onset of recombination (Fig. 7). As recombination proceeds, excitation and recombination with faster electrons smooths the distribution until at 300 fs the irregular structure of the distribution is lost. Some evidence of the discrete nature of the energy levels remains at higher energy. At this time within the upper levels, upward and downward transitions lead to a quasi-thermal balance among their populations. Within this quasi-balance there is a net downward diffusion through the bound states, which eventually leads to the cascade to the ground state.

C. Population

We now examine the effect of recombination on the population of the various hydrogenic states of the lithium ion. We show in Fig. 8(a) the reduced population (q_i/g_i) of each level. It can be seen that the population growth in the levels $n=4$ to $n=10$ is extremely rapid. Due to the rapid rate of transition among these levels, a consequence of electron inelastic collisions, all these levels follow a similar time history. As may be expected the populations of the lower levels are larger than the higher, reflecting the formation of a quasi-thermal distribution among these states. Figure 8(b) shows a Boltzmann plot of the reduced populations in the levels $n=2-10$, compared with the populations derived from Saha's equation and the population of the Li IV next ionization stage at 1 ps and assuming a Maxwellian distribution with temperature given by the mode (7.9 eV). It can be seen that a good thermal balance is maintained down to the level $n=4$, which is the value given by the "bottleneck"
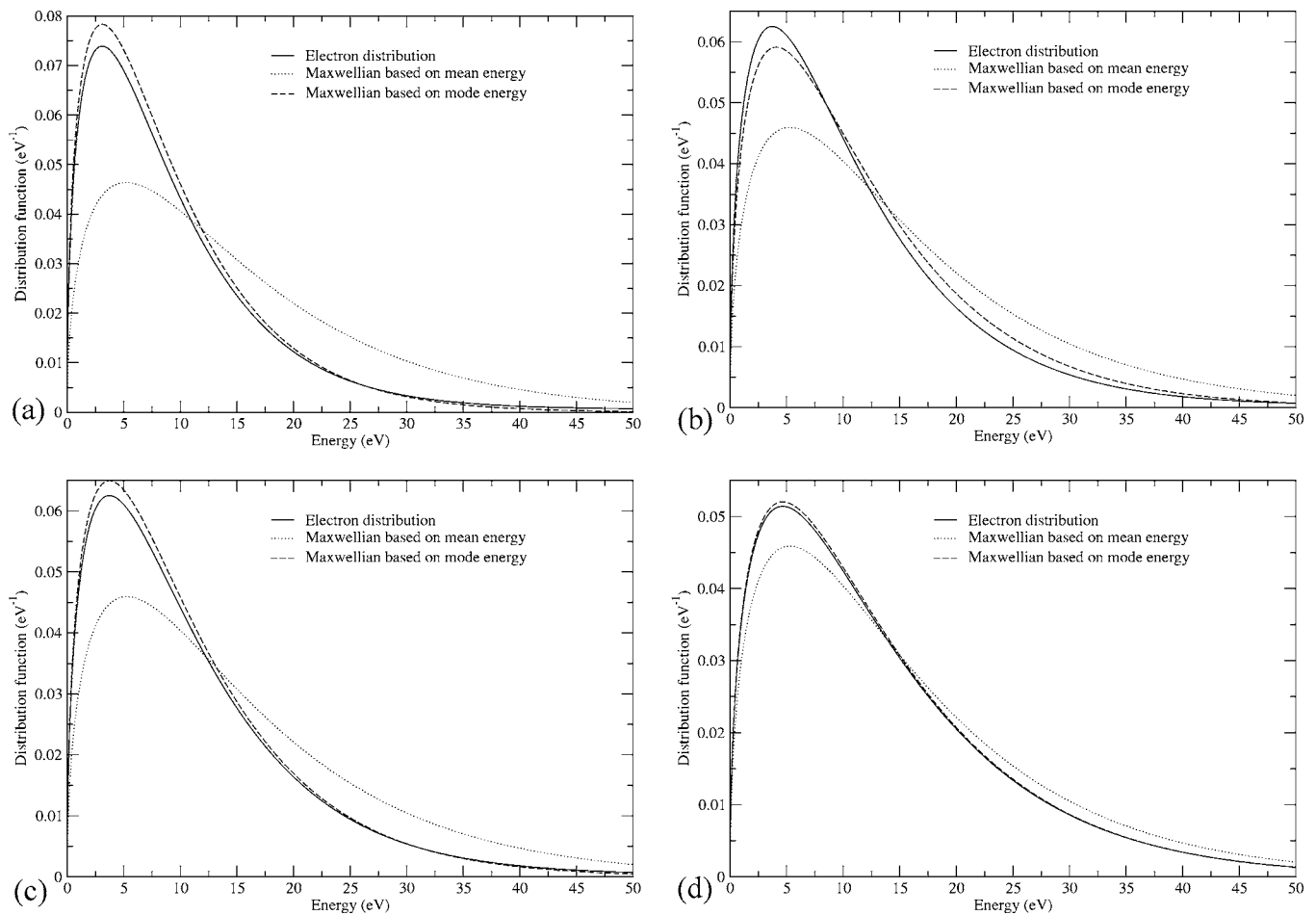
FIG. 4. Plots of the electron distribution function at successive times: (a) 20 fs, (b) 0.5 ps, (c) 1.0 ps, and (d) 2.5 ps after the end of the pulse.

$(n=\sqrt{\{Z^2 I_H/kT_e\}})$ [11]. Thus the electrons are showing classical diffusion through the excited states, which forms the flux leading to the lower state population by cascade. The population of these levels decreases slowly with time due to the removal of the cold free electrons by equilibration and the cascade of electrons through the levels down into the ground state. However, they clearly act as a reservoir supplying the feed into levels $n=3$ and 2, which in turn decay into the ground state.

The populations of the lower levels $n=1$ and 2 show a different behavior reflecting the inability of collisions to strongly populate them directly. They are populated sequentially by both radiative and collisional transitions from the levels above, i.e., by the cascade. In fact collisions are still the dominant transitions as evidenced by the fact that the smaller energy transitions (to the $n=2$ level) occur most rapidly. We, therefore, find a delay between the build-up of population in the resonance $(n=2)$ level and that in the ground state $(n=1)$. This leads to a population inversion, which has quite a substantial density, but is relatively short lived (≈ 0.3 ps). This will lead to gain on the line L_α at 135 Å.

VI. LITHIUM-LIKE NITROGEN (N V)

We turn now to the case considered in our earlier work [2], namely a mixture of nitrogen and hydrogen, in which population inversion can be generated. In this case the active ion is lithium-like. The ground state is $1s^2 2s_{1/2}$ with levels $2p$ at higher energy due to the electron-electron interaction. In these cold plasmas this energy is sufficiently large ≈ 10 eV to allow electron decay from these states to the ground state to be relatively unhindered by excitation. Since the state $2p_{3/2}$ has a radiative transition to the ground state, it is a suitable candidate as the lower laser level. A number of levels are suitable candidates for the upper laser levels, but $3d_{5/2}$ has proved to have the highest gain. This arrangement is in contrast to thermal lasers where the temperature is higher, which use the $3d$ states as the lower laser level and the $4f$ or $5f$ as the upper [32]. The role of the ground state is solely that of a sink accumulating the population as it cascades down through the excited states. The inversions produced are, therefore, at longer wavelength. We use the same computer code, BREAKDOWN, with the same atomic system as in our earlier work [2], including the identical ionization and recombination rates from Moores *et al.* [24]. We consider a mixture of 90% hydrogen and 10% nitrogen with a
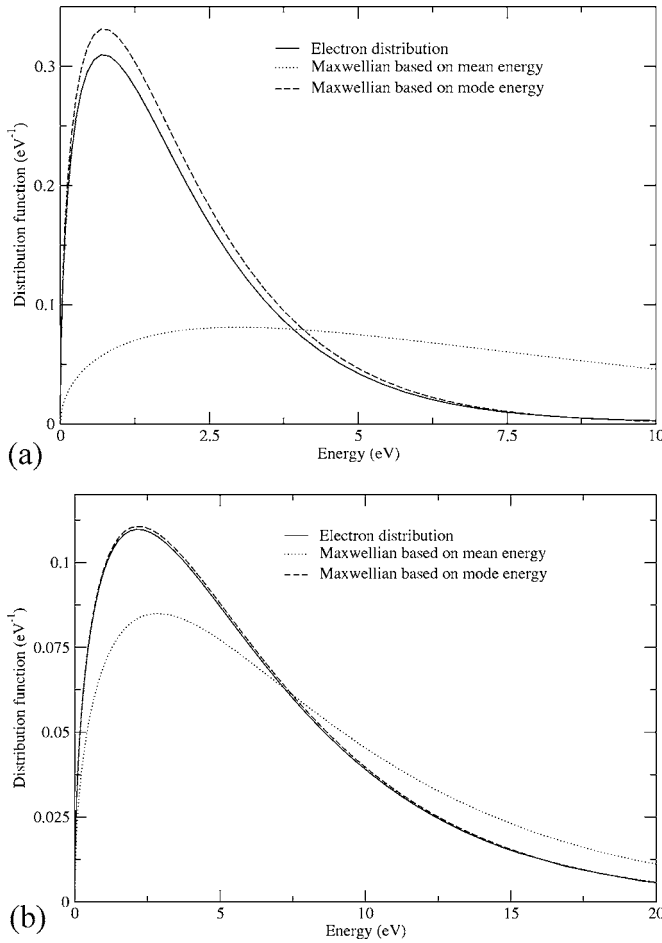
FIG. 5. Plots of the electron distribution function with electron-electron collisions only at times (a) 20 fs and (b) 2.5 ps after the end of the pulse.

total atomic density of 3.5×10^{18} cm^{-3}. The radiation has a wavelength 0.254 μm and an irradiance of 10^{17} W cm^{-2} in a pulse 100 fs duration. This is sufficient to fully ionize the hydrogen and strip the nitrogen to the helium-like ion, N VI.
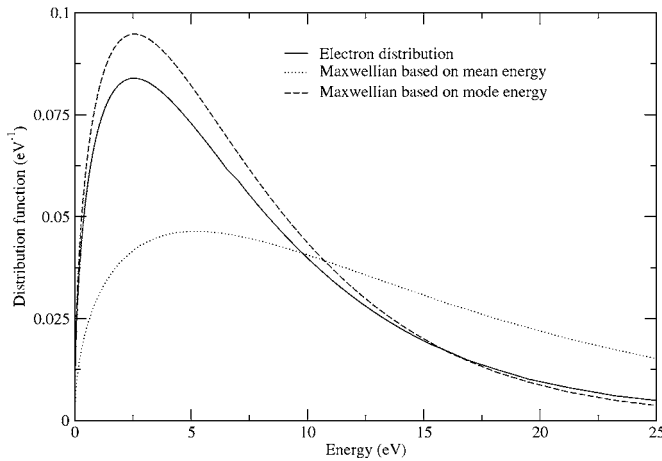

FIG. 6. Electron distribution function with electron-ion collisions only at 0 ps after the end of the pulse.
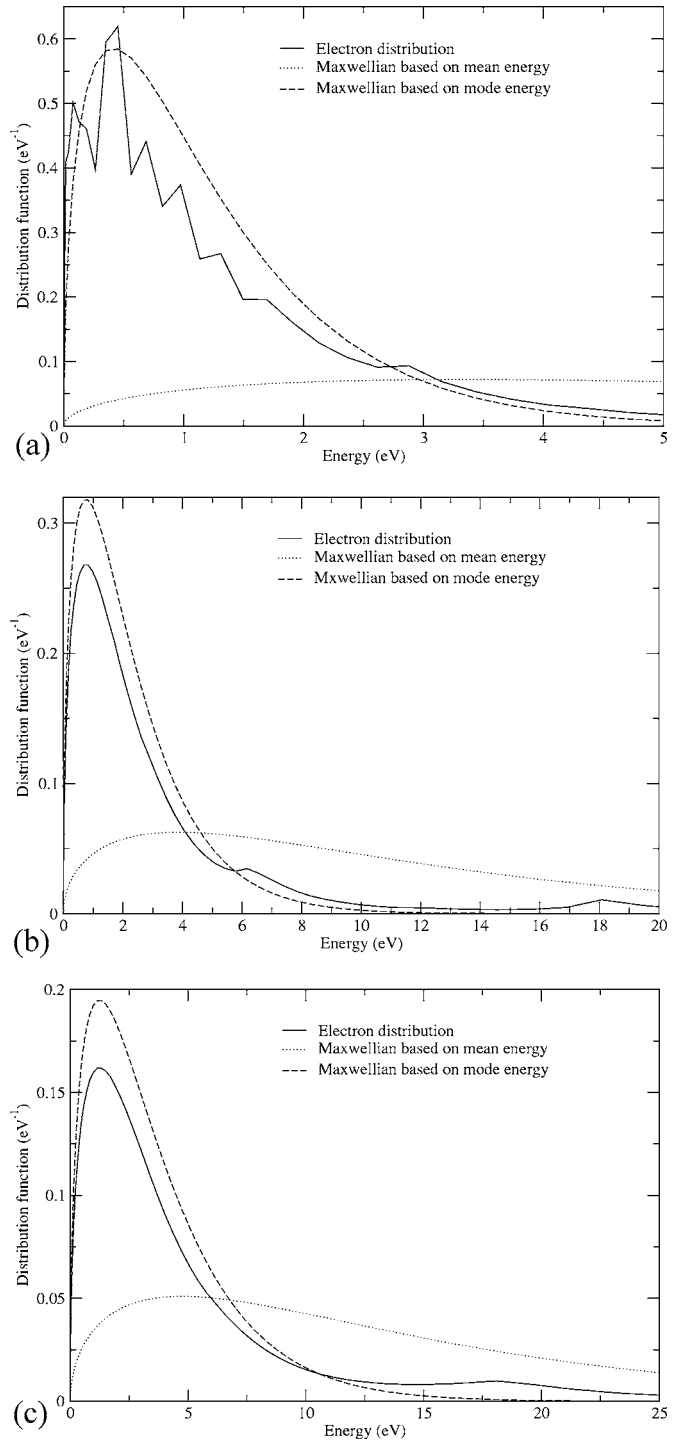

FIG. 7. Electron distribution function following three-body recombination only at (a) 20 fs, (b) 300 fs, and (c) 2.5 ps after the end of the pulse.

A. Electron distribution

In the Fokker-Planck calculations we have used a relatively simple atomic model for the lithium-like nitrogen ion, namely a screened hydrogenic set of states, as a more complete set would have required considerably more computational time, and the results, as we shall see, would not have justified the effort. Figure 9 shows the electron distribution
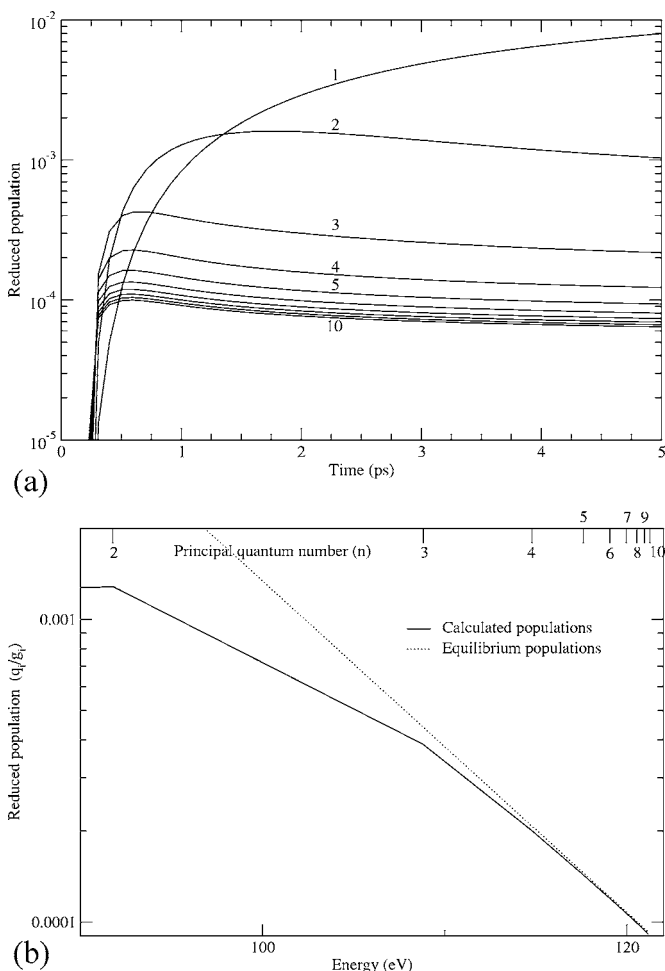
(a)

(b)

FIG. 8. Populations in hydrogen-like lithium (Li III). (a) Li III levels reduced populations as a functions of time. (b) Boltzmann plot of the reduced populations at 1 ps.

(a)

(b)

FIG. 9. Electron distribution function in nitrogen at (a) 20 fs and (b) 300 fs after the end of the pulse.

immediately after and 300 fs after the pulse. In contrast to the lithium case, the electrons are substantially colder and have almost fully relaxed by the end of the pulse. Relaxation is complete by about 1 ps.

This difference is of some interest and may be worthy of a remark. The hydrogen gas density in both the lithium and nitrogen mixtures is the same fraction of the total, and its mean above-threshold ionization (ATI) energy will be the same in each case, namely 0.87 eV per electron. The most important contribution to the difference is due to the variation of the ionization energies of the lasing ions, in the case of lithium (5.39, 75.638, and 122.45 eV) compared to (14.5, 29.6, 47.5, 77.5, and 97.89 eV) for nitrogen. The average ATI electron energy from the lasant is 32.5 eV from lithium, and 4.6 eV for nitrogen. The average energy due to ATI alone is as a result significantly larger from lithium than for nitrogen—8.8 eV compared to 2.3 eV. Inverse bremsstrahlung absorption also makes a larger contribution due to the higher density in the former case. Finally the larger mean energy in lithium gives rise to a substantial "hot" tail in the distribution, whereas the nitrogen distribution is less sharply peaked [cf. Figs. 4(a) and 9(a)]. The larger fraction of low energy electrons in the latter case allows the system to ther-
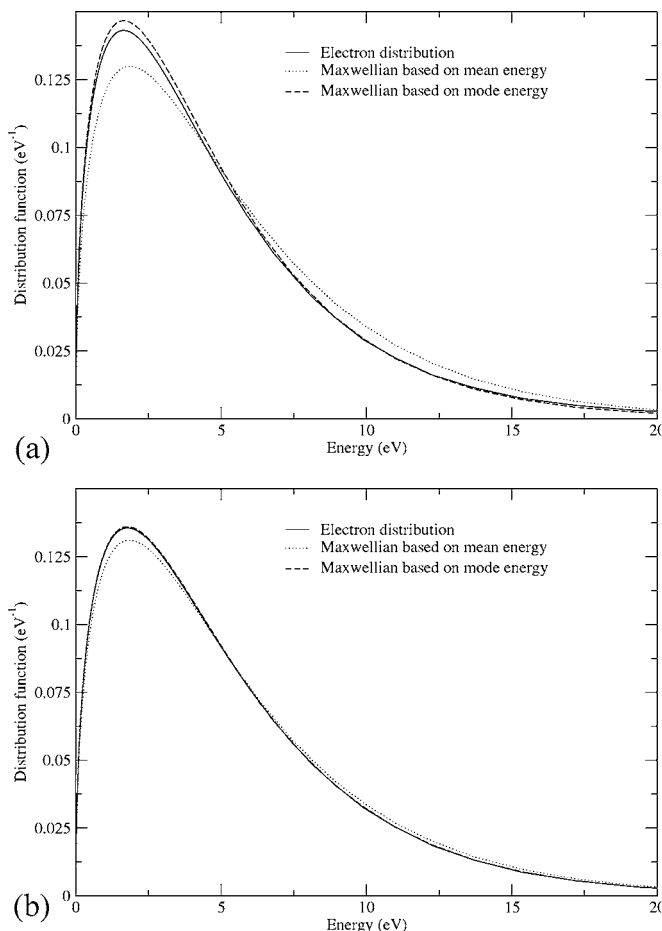
malize more rapidly, and also the equilibration rate is correspondingly increased.

B. Population

The near complete relaxation into a Maxwellian distribution greatly simplifies the calculation of the excited state populations, since thermal rates can be used. We have, therefore, used this approach with a more extensive data set of energy levels than used for the hydrogen-like lithium, taken from our earlier calculations with the same computer model, which uses thermal population rates [2]. In Fig. 10(a) we show the populations of a restricted set of states (not including the ground state) taking one from each principal quantum number shell. The $n=2$ state is the $2p_{3/2}$, which lies 10 eV above the ground state (also $n=2$) and the $n=3$ state the $3d_{5/2}$. These states are the ones showing the highest gain on the line at 249 Å in our earlier simulation. It can be seen that the behavior of the populations of these levels follows the same pattern as that seen in the lithium ion. Population inversion and gain are obtained between the states $n=3$ and $n=2$ almost immediately after the completion of the laser pulse and lasts for about 13 ps until the lower laser level is filled by the cascade. The upper levels show an approximate Boltzmann distribution with the "bottleneck" at about $n=4$.
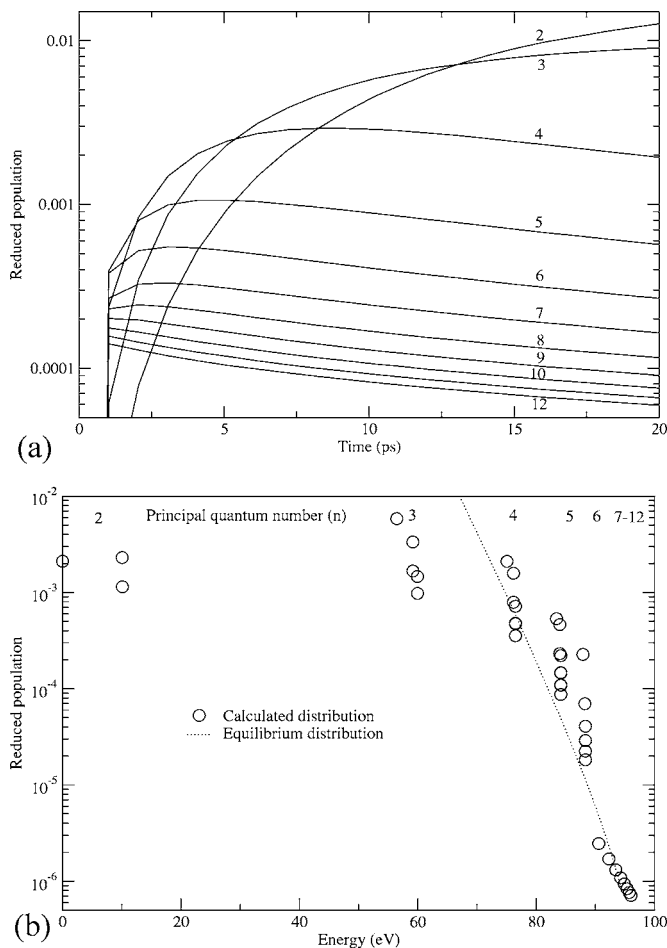
FIG. 10. Populations in lithium-like nitrogen (N V). (a) Populations of the excited states of nitrogen, the index refers to the principal quantum number of the state. (b) Boltzmann plot of the calculated and equilibrium populations of the excited states of nitrogen at 10 ps.

Since the upper laser level in this case is $n=3$, this gives more direct pumping into the lasing states. We observe that the upper laser level $n=3$ does not follow the general behavior of the higher states. We also note that since the effective temperatures are lower than in the lithium case, the populations tend to be more differentiated.

In Fig. 10(b) we show the Boltzmann plot for all 38 levels included in our calculation at 10 ps. The weak inversion between the $n=2$ and $n=3$ levels can be seen, but it will soon be destroyed as the lower levels fill. Unlike the lithium case, the populations do not follow a smooth distribution due to the splitting of the levels $n=2$ to $n=6$. However, the general trend is clear, and can be seen to closely follow the equilibrium line based on the current He-like N VI population and temperature. The departure from equilibrium for levels with $n \leqslant 3$ indicates the bottleneck at $n=4$. Although the electron temperature is only about 4 eV and the hydrogenic formula would indicate that the bottleneck should be at $n \sim 9$, the closer spacing of the actual levels brings the value down to 4. This is a useful feature of the nonhydrogenic systems, which can enhance gain, although at the expense of the shorter wavelength.

VII. DISCUSSION

The plasma generated by tunneling ionization by linearly polarized light has a distribution which is characterized by a large component near zero energy. The plasma as a whole is therefore very cold. The actual shape of the distribution depends quite sensitively on the nature of the ionization structure of the gas and the rise time of the pulse. The distribution may show structure associated with the passage through individual ionization stages. While this is not as apparent as with circularly polarized light, it is nonetheless a significant factor [Fig. 3(a)] and is the reason for seeding the lasant gas with hydrogen, which will ionize early and only generate cold electrons [2].

A complicating factor is that 50% of the ionized electrons may return to the neighborhood of their parent ion where they will be strongly scattered to high energy. At this stage the electron is removed from strong interactions with its fellows or with the ions, i.e., becomes a bystander in the processes of interest. Fortunately at reasonably high densities relatively small deflections by neighboring ions will destroy the coherence of this motion, and the electron will in consequence be only weakly scattered, i.e. absorb a smaller amount of energy similar to inverse bremsstrahlung.

In our analysis we have assumed that the intense laser field which gives rise to tunneling has a negligible effect on the atomic energy levels. Our justification for this is twofold. Firstly the duration of the pulse is very short and during this phase the atoms are assumed to be ionized down to a closed shell (bare nuclei or helium ions), which form an inert core as regards this analysis. During this process it is assumed that only the ground state of each ion is active. No correction is made for any shift of the ground state, which would change the corresponding ionization energy. Secondly it is assumed that the laser switches off rapidly, over times short compared to the onset of recombination. Any residual pulse will ionize the high lying states into which recombination occurs as well as changing their configuration due to a.c. Stark effects. As the laser pulse decreases, the atomic energy levels are assumed to relax back to their field free condition. This allows us to separate the ionization and recombination phases, which are consequently treated independently in the analysis. A more detailed analysis of this process would be of interest, although it is unlikely it would significantly change our conclusions.

The electron distribution is developed through three processes following ionization:

(i) inverse bremsstrahlung during the laser pulse;
(ii) electron-electron collisions;
(iii) three body recombination heating.

We have shown that all three play an important role at the densities we require for sufficient gain to be developed, if working soft x-ray lasers are to be constructed in this manner. All these processes depend on electron-electron or electron-ion collisions, which are much stronger for cold electrons. Therefore the effect of each is similar, namely to drive the low energy part of the distribution into a Maxwellian, whose peak (mode) progressively shifts to higher energy as the hotter electrons are drawn in. Since the cold electrons dominate these processes, their rate can be expressed by a

thermal rate, but with the "temperature" determined by the mode ($kT_e = 2\epsilon_p$).

The electron distribution immediately following ATI will depend strongly on both the ionization structure of the atom and on the pulse rise time of the pump pulse [20]. The pulse rise time should be sufficiently slow that each ionization stage can be ionized near its own threshold field in order to avoid the generation of unnecessary hot electrons, but not long enough to give rise to appreciable inverse bremsstrahlung heating.

The electron distribution is cold and the electron energy is much less that the ground state ionization energy. Three-body recombination is, therefore, dominant into the upper states of the ion, which rapidly achieve an equilibrium distribution with temperature determined by the mode of the free electron distribution. Within these levels, the bound electrons drift up and down in response to excitation/de-excitation collisions with bound electrons of similar energy. The overall drift, however, is down towards the ground state and a fully recombined electron-ion pair. The rate of recombination is, therefore, set by the rate at which electrons drift through the level at which electrons can no longer maintain the upward excitations and only de-excitation can occur. This level can be set either by collisions (bottleneck) or by radiation ("collision limit"). It essentially marks the limit of thermal equilibrium within the excited states.

The importance of the bottleneck and collision limit for recombination pumping were pointed out many years ago by the author [6,33], namely that the upper laser level should lie at or near the limit, and that the lower should be well below. This ensures a good flux of electrons into the upper state, provided recombination and de-excitation within the upper states is rapid. The corresponding rate is the well-known $T_e^{-9/2}$ recombination rate [11]. This condition is established in both our trial systems.

Ground-state lasers were originally proposed in 1972 [7], but were never practicable with traditional expansion-cooled pumping, as the ground state could not be sufficiently well emptied. However, the advent of ATI pumping by short pulse CPA lasers [1] changed that. The original proposal by Eder *et al.* [34] using lithium-like neon is probably not viable, but recently Suckewer and co-workers [4,14] have successfully re-visited the lithium L_α scheme, originally suggested by Nagata *et al.* [35], despite the uncertainty regarding the latter experiments. In our simulations, we have found that population inversion, and consequently gain is practicable, but is short lived. The short lifetime may be a problem as the line width is likely to be very narrow. Consequently the gain lifetime-line-width product may be significantly less than unity, which will reduce the accessible gain. These results are broadly in line with those of Avitzour and Suckewer [14], but they found a significantly longer gain lifetime under their pumping conditions.

Systems not using the ground state, although longer wavelength, avoid this problem as the lower laser state fills more slowly, until an equilibrium is reached with the ground state, as in the case studied here. Excited states used as the lower laser level are the traditional route into recombination pumping where the inversion is formed as a consequence of the transition rates in the cascade down to the ground state.

Lithium-like nitrogen examined here is an exemplar of these systems. In contrast to the lithium system, the electron distribution rapidly equilibrates and the laser behaves similarly to thermal systems, although the lower state is lower than that normally used, where the lower laser state is the $3d$ and the upper either $4f$ or $5f$. The ATI lasers may, however, be limited for practical purposes by their long wavelength and low saturation intensity.

In this paper we have not attempted to use our results for the design of working lasers based on these principles and have, therefore, made no estimates of possible gain resulting from the population inversions. Our reasons for this are two-fold. In the case of the hydrogen-like lithium, the separation of the $n=2$ sub-levels are about 4 meV. Consequently at the density and electron temperature in these experiments these states of common principal quantum number, n, are further split and mixed. Detailed calculation of the gain may be complicated and require a more detailed analysis of the individual states [36]. In our calculations we have assumed that the states are fully mixed. For lithium-like nitrogen, these problems do not arise and we have already presented detailed calculations of gain elsewhere [2].

Throughout this work we have assumed that dilute weakly coupled plasma theory is appropriate despite the low temperature and relatively high densities. For the lithium system, where $Z^* \approx 1.2$, $n_e \approx 1.2 \times 10^{19}$ cm^{-3}, and $T_e \approx 7.9$ eV, we find that the Debye length $\lambda_D \approx 5.8 \times 10^{-7}$ cm and the ion sphere radius $R_0 \approx 2.9 \times 10^{-7}$ cm, the strong coupling parameter is thus $\Gamma = Z^{*2}\lambda_D/R_0 \approx 2.2$. Similarly for nitrogen we have $Z^* \approx 1.4$, $n_e \approx 4.9 \times 10^{18}$ cm^{-3}, and $T_e \approx 3.5$ eV so that $\lambda_D \approx 6.3 \times 10^{-7}$ cm, $R_0 \approx 4.1 \times 10^{-7}$ cm, and $\Gamma \approx 2.3$. These systems, therefore, lie at the borderline of strongly coupled plasmas. In the present context, ion-ion correlations are unimportant as the ions are assumed fixed over the short time scales of the calculation. The ions, therefore, retain the original random positions of their parent atoms: A result consistent with weak ion-electron thermalization calculated for nitrogen using the BREAKDOWN code.

More serious is the effect on the electron-electron collisions of the result that the ion sphere radius is less than the Debye length $R_0 < \lambda_D$. In principle this may violate our condition of weak collisions implicit in the Fokker-Planck model. However, provided this radius is still large compared to the inner "cutoff" distance—the larger of the electron wavelength and the Landau length—the majority of the collisions are still weak, but the outer cutoff should be taken as the ion sphere radius rather than the Debye length. Fortunately in this case there is little difference between the two, as the term is only used logarithmically. Estimating the inner cutoff we find that for the lithium simulations the Landau length $b_{min} \approx 2.3 \times 10^{-8}$ cm and the electron wavelength $\lambda_e \approx 2.8 \times 10^{-8}$ cm, and for nitrogen $b_{min} \approx \lambda_e \approx 5.8 \times 10^{-8}$ cm. The condition of validity is thus upheld, although perhaps not as strongly as one would wish. This limitation can be overcome by either molecular dynamics [19] or Monte Carlo [20] calculations but only at the expense of a very substantially increased computational effort.

There is one further effect of dense plasmas, which should be examined, namely the depression of the ionization level, which will be determined by the inter-particle separation. We

note that since an equilibrium is assumed between the high lying bound states and the continuum in our model of cascade recombination, the exact nature of these states will play little role. However, if we recall that the radius of the Bohr orbits scate as $a_0 n^2/Z$ where Z is the ion-core charge and $a_0 = 0.532 \times 10^{-8}$ cm the Bohr radius, we see that the electrons are bound for $n \lesssim 12$ for lithium and $n \lesssim 21$ for nitrogen. We may remark that this depression of ionization is included in the code BREAKDOWN used in the calculations for the nitrogen ions using the thermal picture, where bound states are found at $n = 12$ [Fig. 10(b)].

The calculations using our Fokker-Planck model have only considered recombination resulting from radiative and three-body capture. We have not included di-electric recombination or other effects. Clearly di-electronic recombination is only important for lithium-like plasmas, and is included in our more general thermal code BREAKDOWN using a screened hydrogenic atom model. Calculations show that it plays little role in the cases discussed here.

One further observation concerns the choice of density. Clearly high density improves the gain directly through the number of inverted ions present, although since it also increases the linewidth through Stark broadening this may be somewhat mitigated. The pumping rate due to recombination will increase through the n_e^2 scaling. But increasing density also increases the inverse bremsstrahlung absorption rate during the laser pulse, and increases the temperature. Since the recombination rate scales as $T_e^{-9/2}$, this can be seriously damaging. As a rough guide the density should not exceed the value at which the inverse bremsstrahlung energy gain equals the ATI energy. However, in assigning this limit, care must be taken to avoid some of the potential pitfalls noted above.

[1] N. Burnett and P. Corkum, J. Opt. Soc. Am. B **6**, 1195 (1989).

[2] M. Grout, K. Janulewicz, S. Healy, and G. Pert, Opt. Commun. **141**, 213 (1997).

[3] T. Ditmire, Phys. Rev. E **54**, 6735 (1996).

[4] Y. Avitzour, S. Suckewer, and E. Valeo, Phys. Rev. E **69**, 046409 (2004).

[5] P. Jaeglé, G. Jamelot, A. Carillon, A. Sureau, and P. Dhez, Phys. Rev. Lett. **33**, 1070 (1974).

[6] G. Pert, J. Phys. B **9**, 3301 (1975).

[7] J. Peyraud and N. Peyraud, J. Appl. Phys. **43**, 2993 (1972).

[8] E. Hinnov and J. Hirshberg, Phys. Rev. **125**, 795 (1962).

[9] L. Pitaevskii, Sov. Phys. JETP **15**, 913 (1962).

[10] H. Griem, *Plasma Spectroscopy* (McGraw-Hill, New York, 1964).

[11] G. Pert, J. Phys. B **25**, 619 (1990).

[12] R. Jones and K. Lee, Phys. Fluids **25**, 2307 (1982).

[13] P. B. Corkum, Phys. Rev. Lett. **71**, 1994 (1993).

[14] Y. Avitzour and S. Suckewer, J. Opt. Soc. Am. B **23**, 925 (2006).

[15] G. Pert, J. Phys. B **34**, 881 (2001).

[16] M. Rosenbluth, W. MacDonald, and D. Judd, Phys. Rev. **107**, 1 (1957).

[17] S. Chandrasekhar, *Principles of Stellar Dynamics* (Dover, New York, 1960).

[18] W. Thompson, *An Introduction to Plasma Physics* (Pergamon, Oxford, 1962).

[19] N. David and S. M. Hooker, Phys. Rev. E **68**, 056401 (2003).

[20] G. Pert, J. Phys. B **32**, 27 (1999).

[21] L. Landau and E. Lifshitz, *Quantum Mechanics* (Pergamon, Oxford, 1959).

[22] W. Lotz, Z. Phys. **232**, 101 (1970).

[23] A. Burgess and I. Percival, Adv. At. Mol. Phys. **4**, 109 (1968).

[24] D. Moores, L. Golden, and D. Sampson, J. Phys. B **13**, 385 (1980).

[25] G. Wannier, Phys. Rev. **90**, 817 (1953).

[26] A. Burgess, in *Proc. Sym. Atomic Collision Processes in Plasmas* (Culham Lab, U.K.A.E.A, 1964), 4818, pp. 63–71.

[27] A. Perelomov, V. Popov, and M. Terentév, Sov. Phys. JETP **23**, 924 (1966).

[28] M. Ammosov, N. Delone, and V. Krainov, Sov. Phys. JETP **64**, 1191 (1986).

[29] G. Paulus, W. Becker, W. Nicklich, and H. Walter, J. Phys. B **27**, L703 (1994).

[30] M. Smirnov and V. Krainov, J. Phys. B **31**, L519 (1998).

[31] N. Delone and V. Krainov, J. Opt. Soc. Am. B **8**, 1207 (1991).

[32] G. Jamelot, A. Klisnick, A. Carillon, H. Guennou, A. Sureau, and P. Jaeglé, J. Phys. B **18**, 4847 (1986).

[33] G. Pert and S. Ramsden, Opt. Commun. **11**, 270 (1974).

[34] D. C. Eder, P. Amendt, and S. Wilks, Phys. Rev. A **45**, 6761 (1992).

[35] Y. Nagata, K. Midorikawa, S. Kubodera, M. Obara, H. Tashirto, and K. Toyoda, Phys. Rev. Lett. **71**, 3774 (1993).

[36] A. Borovskiy, P. Holden, M. Lightbody, and G. Pert, J. Phys. B **25**, 4991 (1992).